Chemical Geology 499 (2018) 58–70

Contents lists available at ScienceDirect

Chemical Geology

journal homepage: www.elsevier.com/locate/chemgeo

High-resolution reconstruction of historical flood events in the Changjiang River catchment based on geochemical and biomarker records

Rui Zhang[a,b,c,d,e,*,1], Tiegang Li[f,g,h,**,2], James Russell[d,3], Yurou Zhou[i,4], Fan Zhang[i,4], Zhiyong Liu[j,5], Minglei Guan[b,6], Qi Han[k,7]

[a] Jiangsu Key Laboratory of Marine Bioresources and Environment, Huaihai Institute of Technology, Lianyungang 222005, Jiangsu Province, China
[b] School of Geodesy and Geomatics Engineering, Huaihai Institute of Technology, Lianyungang 222005, Jiangsu Province, China
[c] Key Laboratory of Marine Geology and Environment, Institute of Oceanology, Chinese Academy of Sciences, Qingdao 266071, China
[d] Department of Earth, Environmental, and Planetary Sciences, Brown University, Providence, RI 02912, USA
[e] Co-Innovation Center of Jiangsu Marine Bio-industry Technology, Huaihai Institute of Technology, Lianyungang 222005, Jiangsu Province, China
[f] First Institute of Oceanography, State Oceanic Administration, Qingdao 266061, Shandong Province, China
[g] Laboratory for Marine Geology, Qingdao National Laboratory for Marine Science and Technology, Qingdao 266061, China
[h] University of Chinese Academy of Sciences, Beijing 100049, China
[i] Department of Chemical Engineering, Huaihai Institute of Technology, Lianyungang 222005, Jiangsu Province, China
[j] School of Radiation Medicine and Protection, Medicine College, Soochow University, Suzhou 215021, Jiangsu Province, China
[k] School of Ocean Sciences, China University of Geosciences, Beijing 100083, China

ARTICLE INFO

Editor: G. Jerome

Keywords:
East China Sea
BIT
BrGDGTs
Sr-Nd isotope
Marginal Sea
Sediment geochemistry

ABSTRACT

Extreme hydrologic events such as floods have caused catastrophic losses to modern human society, especially in highly developed coastal areas. However, high-resolution reconstructions of extreme flood events are scarce due to a paucity of suitable proxies in marginal seas. Here we present a high-resolution record of extreme flood events in the Changjiang River catchment during the last 110 years using samples from the subaqueous delta of Changjiang River estuary. We used a multi-proxy approach including Sr-Nd isotopes, Zr/Rb ratio and biomarkers (branched GDGTs, i.e. brGDGTs, and crenarchaeol, and the ratio of the two as calculated by the BIT index) as proxies for the evolution of extreme floods in the Changjiang River catchment. Rapid shifts in these proxies agreed with the timing of floods on the Changjiang River. We also tested the reliability of biomarker indices to reconstruct paleoflood events in this area. The results indicated that the abundances of GDGTs fluctuated in concert with historical floods. Cross-spectral analyses revealed that historical floods in the Changjiang River catchment were consistent with ENSO variance.

1. Introduction

Large river estuaries are important interfaces between continents and the oceans and record environmental changes in their rapidly accumulating sedimentary archives. These archives include valuable information of variability in climate and land-use in catchments, the frequency and magnitude of extreme weather events such as cyclones and floods, as well as sea-level changes. With a length of approximately 6300 km, the Changjiang River, or the Yangtze River, is the longest river in Asia. The Changjiang River is home to 400 million people and delivered 500 Mt/yr of sediment to the East China Sea (ECS) prior to the 1970s (Liu et al., 2007). However, there has been a 70% reduction (to 150 Mt/yr) in Changjiang River's sediment reaching the delta over recent decades due to dam trapping (Yang et al., 2014, 2015a). The

* Correspondence to: R. Zhang, School of Geodesy and Geomatics Engineering, Huaihai Institute of Technology, 222005, Jiangsu Province, China.
** Correspondence to: T. Li, First Institute of Oceanography, State Oceanic Administration, 266061 Qingdao, China.
E-mail addresses: rzhang_838@163.com (R. Zhang), tgli@fio.org.cn (T. Li).
[1] Institutional mailing address: No. 59, Cangwu Road, Xinpu District, Lianyungang, Jiangsu Province, China
[2] Institutional mailing address: No. 6, Xianxialing Road, Laoshan District, Qingdao, Shandong Province, China
[3] Institutional mailing address: 324 Brook Street, Providence, RI 02912, USA
[4] Institutional mailing address: No. 59, Cangwu Road, Xinpu District, Lianyungang, Jiangsu Province, China
[5] Institutional mailing address: No. 199, Renai Road, Industrial Park District, Suzhou, Jiangsu Province, China
[6] Institutional mailing address: No. 59, Cangwu Road, Xinpu District, Lianyungang, Jiangsu Province, China
[7] Institutional mailing address: No. 3, Xueyuan Road, Haidian District, Beijng, People's Republic of China

https://doi.org/10.1016/j.chemgeo.2018.09.003
Received 30 January 2018; Received in revised form 20 August 2018; Accepted 3 September 2018
Available online 13 September 2018
0009-2541/

Changjiang River basin has also experienced numerous extreme flood events, which caused casualties and economic losses in the last century (Li and Zhang, 2004; Yuan et al., 2006). Hence, it is important to understand the mechanisms influencing extreme flood events in eastern China, which will also assist in predicting future climate changes.

Recent work has shown the Changjiang River has accumulated 1200×10^9 t of sediment in its deltaic plain and subaqueous estuary during Holocene (Liu et al., 2007). These sediments have been trapped on the inner shelf due to a variety of hydrodynamic processes, forming muddy areas on the subaqueous delta and the Zhe-Min coastal mud area (DeMaster et al., 1985; Liu et al., 2007; Guo et al., 2007; Xu et al., 2012). High-resolution sedimentary sequences from these muds can provide opportunities to investigate in detail the complex interplay between sedimentation in the continental margin, climate, and anthropogenic activities in one of the largest river systems in the world. Despite potential of such, it remains challenging to associate sediment grain size and some geochemical proxies (e.g. Zr/Rb ratio) (Zhang et al., 2009; Wang et al., 2011; Hu et al., 2014; Zhao et al., 2016), whereas sediment grain sizes are easily affected by estuarine hydrodynamic processes. However, few researches focused on the high-resolution reconstruction of extreme climatic events (e.g., floods) in coastal regions of the ECS based on the multi-proxy approach. Testing powerful multi-proxy (e.g. Sr-Nd isotopes, Zr/Rb ratio and biomarkers) against historic records of palaeo-flood events is desirable.

Two such complementary proxies include radiogenic Sr and Nd isotopes and microbial biomarkers. Sr and Nd isotopes are powerful tools to fingerprint the sources of fluvial sediments (Smith et al., 2003; Grousset and Biscaye, 2005; Singh et al., 2008; Chen et al., 2007; Yang et al., 2007; 2015b; Li et al., 2015a; Bi et al., 2017; Pradhan et al., 2017). Seasonal variations of these isotopic signatures in riverine sediments from the Changjiang River are strongly affected by the monsoon climate (Mao et al., 2011; Luo et al., 2012). The branched and isoprenoid tetraether (BIT) index is also a potential proxy to track river-borne soil and sediment sources (Huguet et al., 2007; Kim et al., 2009, 2014; Smith et al., 2010). The BIT index is based on the abundances branched glycerol dialkyl glycerol tetraethers (brGDGTs) derived from bacteria (Weijers et al., 2006) that occur widely in soil (Weijers et al., 2007), versus an isoprenoidal GDGT, crenarchaeol, produced predominantly by marine planktonic Group I Crenarchaeota (Schouten et al., 2013a, 2013b). Variation in the concentration of brGDGTs in surficial continental shelf sediments may be correlated to soil inputs from the Changjiang River basin (Zhu et al., 2011). The BIT index of surface sediments decreases from the estuary and subaqueous delta to the outer shelf of ECS (Zhu et al., 2011, 2013; Lv et al., 2015). Thus, the BIT index may be applied to reconstruct flood events in the estuary and subaqueous delta of the Changjiang River. In this study, two sediment cores from different regions of the subaqueous delta of the Changjiang River were used to examine changes in sedimentary archives as they relate to paleofloods. We presented high-resolution sedimentary records of Sr-Nd isotopes, Zr/Rb and the BIT index spanning the last 110 years in order to investigate the linkage between historical sedimentary records and extreme climate events (e.g., floods) in the coastal regions of ECS. This work sets the stage to develop longer flood records as new sediment cores become available.

2. Regional setting

The Changjiang River (Yangtze River), is the largest river in China. With adrainage basin area of 1.8×10^6 km^2 and an average water discharge of 9.2×10^{11} m^3/yr, it is the 3rd and 5th largest in the world in terms of drainage basin area and water discharge, respectively. It originates in the Tibetan Plateau at an elevation of 6600 m and flows to the east where it discharges into the ECS. Geologically, the Changjiang River catchment is characterized by complex rock compositions, including Paleozoic carbonate rock, Jurassic red sandstone, Mesozoic igneous rocks, Paleozoic marine and Quaternary fluviolacustrine sedimentary rocks (Yang et al., 2004). This catchment can be divided into five broad physiographic provinces, including the northeast Tibetan Plateau, the high mountains of the Longmen Shan and associated ranges, the Sichuan Basin, mixed mountain and basin terrains (broadly referred to as the Three Gorges area), and the eastern lowlands. Generally, the Changjiang River can be divided into three parts: upper, middle, and lower reaches. However, the upstream reaches can further be divided into two segments: the Jinshajiang and the Chuanjiang (He et al., 2015; Bi et al., 2017). The Changjiang River drainage covers several tectonic units, with the main body of the Yangtze Craton and the Qamdo Block, the Songpan-Garze terrane, the Qinling-Dabie orogenic belts, and the Cathaysia Block forming the primary potential sources (He et al., 2015).

The fluvial discharge to the ECS is controlled by rainfall on the Chinese continent, which is largely driven by the East Asian Summer Monsoon (EASM), and also impacted by the Indian Summer Monsoon (ISM) (Xu et al., 2012; Zhao et al., 2015). The EASM prevails across the catchment, resulting in uneven rainfall over the basin at a seasonal scale, with approximately 87% of its annual water and sediments discharges during the flood season (June to October) (Guo et al., 2007; Yang et al., 2015a). Previous research has found that severe floods in the watersheds of Changjiang River can be attributed to the interannual and interdecadal variations of the EASM (Yang et al., 2011; Huang et al., 2007). Heavy rainfall over the Changjiang River catchment is usually accompanied by a weak EASM, which may strengthen the convergence and ascending motions of water vapor along the front of Plum Rains (Huang et al., 2007). The catchment of Changjiang River is known for its frequent huge floods that have limited development within the basin, especially in the middle and lower catchments (Zhao, 2000; Cai et al., 2001; Yu et al., 2009). Over the last century, there are the two major flood recurrences intervals (16.4 years and 2.5 years), as revealed by the mean discharge in the Changjiang River (Yu et al., 2009). Major floods in the Changjiang River catchment are thought to have increased in the recent decades (Jiang et al., 2007). The highest discharge increased from $< 6.6 \times 10^4$ m^3/s before 1950s to $> 7.0 \times 10^4$ m^3/s after 1950s at Hankou hydrological gauge station (Yu et al., 2009). Indeed, it reached 7.6×10^4 m^3/s in 1954 at Hankou (Jiang et al., 2007; Yu et al., 2009). During 1865–2000, six high magnitude floods were recorded at Hankou station, respectively in the year of 1870, 1931, 1935, 1954, 1995 and 1998. The peak water level increased from 27.36 m in 1870 to 29.73 m in 1954, and to 29.43 m in 1998 (Jiang et al., 2007; Yu et al., 2009). The peak water level of 4 m at Nanjing hydrological gauge station is treated as the threshold of local flood occurrence (JPHWRIB, 2016).

Due to the migration of monsoon rainfall within the watershed, Changjiang sediment discharge into the ECS has variable sources in different seasons (Mao et al., 2011; Luo et al., 2012). This suspended sediment is subject to strong tidal action, in addition to the shelf and estuarine circulation (Milliman and Farnsworth, 2013; DeMaster et al., 1985). Approximately 40% of the Changjiang sediment discharge is thought to escape the estuary, and be deposited on the inner shelf north of 30°N, where the mud deposits of the deltaic front facies are found (DeMaster et al., 1985). During flood events, the sediment deposited differs from normal deposits in sediment structure, and physical and geochemical characteristics, differences that can be used as proxies to identify flood events in sediment cores.

3. Materials and methods

3.1. Samples collection

Two sediment cores were collected from the subaqueous delta of the Changjiang estuary in Jul 2015 (Fig. 1), using a gravity corer, and are referred to here as YE-1 (122.35°E, 31°N, water depth 13 m) and DH-1(123°E, 30°N, water depth 61 m). The length of the two sediment cores was 140 cm. YE-1 and DH-1 were sub-sampled at 1 cm intervals, and

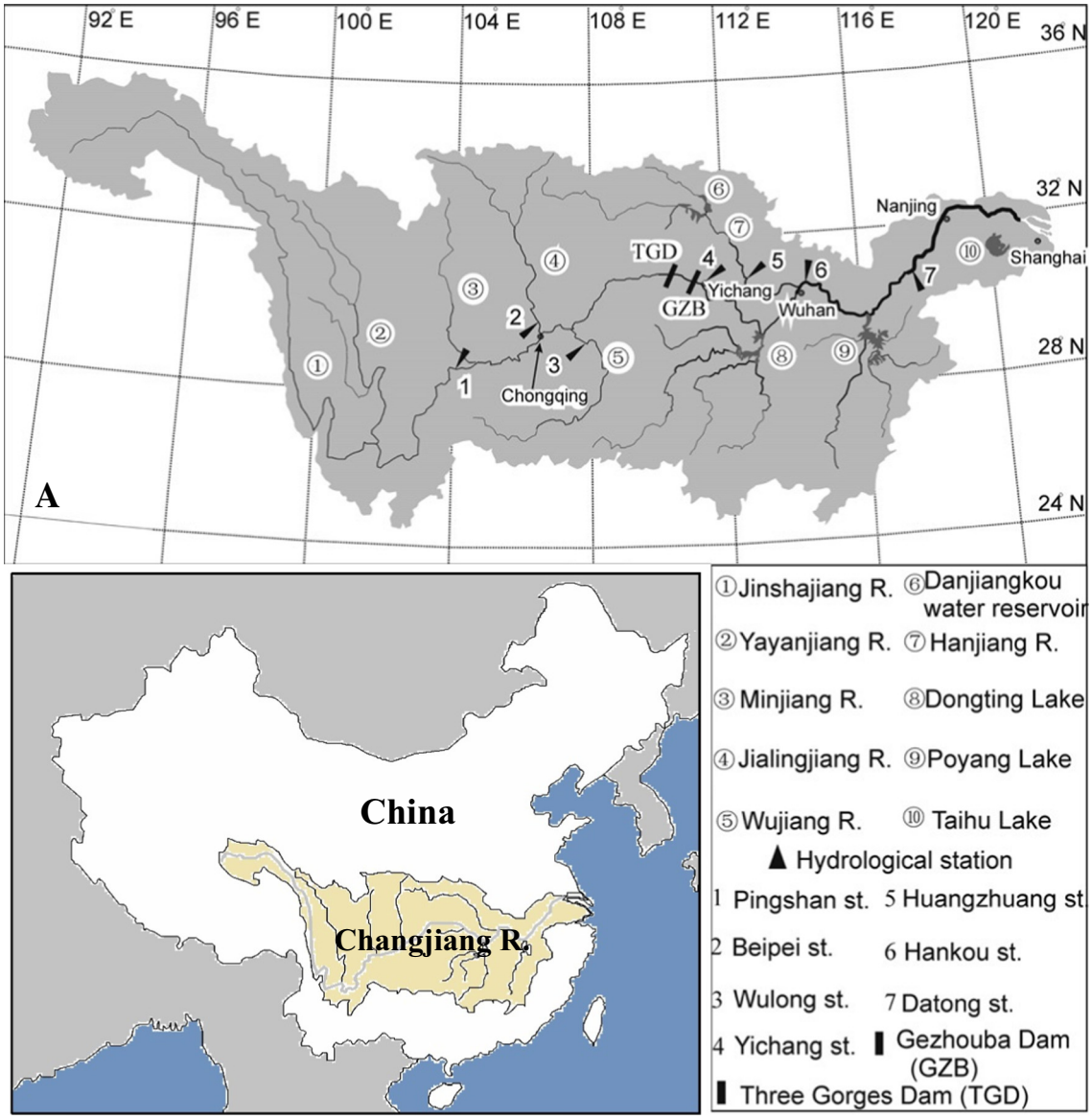

Fig. 1. Study area and locations of sediment cores and suspended sediment samples. (A) Changjiang (Yangtze) River Basin; (B) locations of cores. The red dashed line represents the delineations of the Changjiang subaqueous delta (Yang et al., 2015b; Gao et al., 2016). JWC-Jiangsu Coastal Currents; ZFCC-Zhejiang-Fujian Coastal Currents; YSWC-Yellow Sea Warm Currents; TWC-Taiwan Warm Current; KC-Kuroshio Current. (For interpretation of the references to color in this figure legend, the reader is referred to the web version of this article.)

the sub-samples were then frozen until further analysis. From Jul 2015 to Sep 2016, 14 suspended sediment samples (SSS) were collected at Xuliujing near the Changjiang River estuary. All SSSs were collected from the middle of the river depth in the main river channel of the Changjiang River, with an average depth of 23 m.

3.2. Grain size analysis

Grain size measurements were conducted according to Yu et al. (2014). Wet sediment was treated sequentially with 10% H_2O_2 and 1 mol/L HCl to remove organic matter and carbonate. The grain-size analyses were undertaken using a Mastersizer 2000 laser particle analyzer (with measurements ranging from 0.02 to 2000 μm). Clay (> 8Φ), silt (4 Φ–8Φ) and sand (< 4Φ) fractions were calculated from the cumulative grain size distributions based on percent volume.

3.3. Total organic carbon (TOC) and radionuclides (^{210}Pb, ^{137}Cs and $^{239+240}$Pu) analysis

0.5 g sediment subsamples were decarbonated with 5–10 ml 2 M HCl at room temperature for 12 h then rinsed with deionized water four times (Yu et al., 2015). The decarbonated samples were then freeze-dried and transferred into tin capsules. %TOC was measured using a Euro EA 3000 Elemental Analyzer (Thermal, USA), with a standard deviation of ± 0.02% dry wt (n = 5) for %TOC.

For radionuclide analysis, 30–50 g subsamples were sealed in 40 mm diameter Petri dishes and allowed to sit for a minimum of 21 days to allow ^{210}Pb activities to achieve to secular equilibrium. ^{210}Pb and ^{137}Cs were measured by γ-spectrometry. Total ^{210}Pb activities were determined from the 46 keV photopeak, and supported ^{210}Pb activities were determined by using averaged activities of the ^{226}Ra daughter products ^{214}Pb (295 and 352 keV) and ^{214}Bi (609 keV). ^{137}Cs activities were determined from the 661.62 keV photo peak. The counting system is equipped with a 40% efficiency HPGe detector (GMX30P-A, ORTEC)

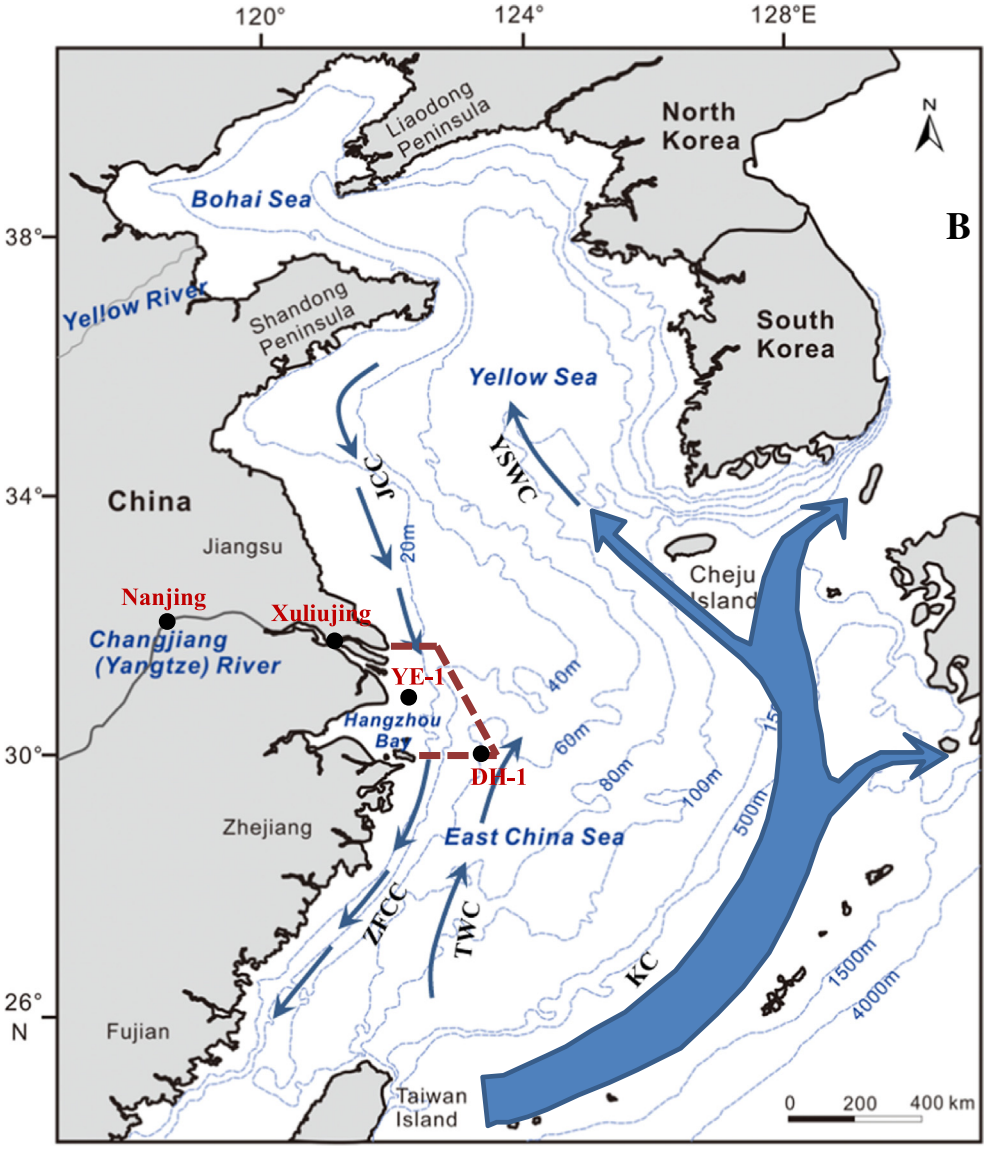

Fig. 1. (*continued*)

interfaced to a digital γ-ray spectrometer (ORTEC DSPEC Plus™). IAEA-327 and a sediment standard supplied by Bedford Institute of Oceanography were used to calibrate the detector.

Approximately 2–3 g subsamples were taken for Pu isotopic analysis. Details of sample pretreatment, chemical separation and purification for Pu isotopes determination have been described elsewhere (Zheng and Yamada, 2006). Pu analysis was conducted by Sector-Field-ICP-MS (Finnigan Element 2, Bremen, Germany) using the method described by Zheng and Yamada (2006). The detection limits for Pu isotopes were found to be 0.0006 mBq/g for ^{239}Pu and 0.003 mBq/g for ^{240}Pu, calculated for 1 g of sediment sample. Reference materials of IAEA-368 and NIST-4357 were used for the analytical method validation.

3.4. Elemental concentrations

About 0.5 g subsamples were placed into Teflon pots, and mixed with nitric acid and hydrofluoric acid, as described by Li et al. (2015a). These mixtures were transferred to a sealed container and heated on a hot plate at 150 °C for 24 h. Then, the hot plate was cooled to 120 °C and perchloric acid was added, and samples were dried with containers opened. The resultant cake was cooled and dissolved in cold nitric acid. Concentrations of trace elements (i.e. Rb and Zr) were determined by an inductively coupled plasma mass spectrometer (Thermo Element XR) in the Institute of Geophysical and Geochemical Exploration, Chinese Academy of Geological Sciences. The differences between measured and certified elemental concentrations of national geo-standards (GSS2, GSS24, and GSD9) were always < 5%. The recoveries of measured total concentrations were estimated to be above 90%. The analytical precision on replicate measurements is generally better 3% for trace elements.

3.5. Sr-Nd isotopic analyses

Total of 97 sediment samples were respectively collected from cores YE-1 and DH-1, as well as 14 suspended sediment samples from Xuliujing, for the measurement of Sr-Nd isotopes. Detrital fractions of these samples were obtained following the methods of Bayon et al. (2002) and Li et al. (2015a). Briefly, the bulk sediment was treated using several reagents (deionized water, 10% HOAc, a mixture of 1 mol/L NH_2·OH·HCl and 25% HOAc, 5% H_2O_2, and 2 mol/L Na_2CO_3) to remove sea salt, calcium carbonate, authigenic components, organic compounds, and biogenic silica, respectively. The resulting detrital fractions were completely digested and concentrated. The measurement

of $^{87}Sr/^{86}Sr$ and $^{143}Nd/^{144}Nd$ ratios were determined using a thermal ionization mass spectrometer (GV ISOPROBE-T) in the Analytical Laboratory Beijing Research Institute of Uranium Geology, with the same analytical method and accuracy for Sr-Nd isotopes reported by Li et al. (2015a). Standards (NBS SRM987 Sr standard) and Shin Etsu JNdi-1 Nd standard were used to monitor analytic error, and their measured values of $^{87}Sr/^{86}Sr$ ratios were 0.710257 ± 21 (n = 11, 2SD) and $^{143}Nd/^{144}Nd$ ratios were 0.512141 ± 9 (n = 6, 2SD), respectively. Sr-Nd isotopic results were normalized to a SRM987 $^{87}Sr/^{86}Sr$ value of 0.710250 and a JNdi-1 $^{143}Nd/^{144}Nd$ value of 0.512115, respectively (Tanaka et al., 2000). For convenience, the $^{143}Nd/^{144}Nd$ ratio is expressed as εNd relative to the Chondritic Uniform Reservoir value of 0.512638 (Jacobsen and Wasserburg, 1980).

3.6. GDGT analysis and BIT calculation

GDGT analysis was conducted following the protocol described in Ge et al. (2014) and Xing et al. (2014). About 5 g of sediment samples were spiked with a quantified standard (C_{46} GDGT) (Huguet et al., 2006) and extracted ultrasonically for 15 min with a dichloromethane/methanol mixture (DCM/MeOH, 3:1, v/v; 5×) and MeOH (1×). With each extraction, the sample was centrifuged at 3000 rpm for 3 min to remove particles. All supernatants were combined. The total lipid extract (TLE) was condensed to 1–2 ml under a N_2 stream. GDGT cleanup was performed using an activated Al_2O_3 column in which each TLE was separated into apolar and polar fractions with hexane and DCM/MeOH (1:1; v/v), respectively. The polar fraction (containing GDGTs) was condensed to 1–2 ml under N_2 and passed through a 0.45 μm PTFE filter to remove particles. The final solution was dried under N_2. The dried polar fraction was dissolved in 300 μl hexane/isopropanol (99:1; v/v) prior to injection. GDGT analysis was conducted using high performance liquid chromatography-mass spectrometry (HPLC-MS, Agilent 1200) with atmospheric pressure chemical ionization (APCI), equipped with an autosampler and ChemStation manager software. GDGTs were eluted at 0.2 ml/min with hexane/isopropanol (99:1; v/v) for the first 5 min, then with a linear gradient up to 1.8% isopropanol in 45 min in normal phase with a Prevail Cyano column (150 × 2.1 mm). The MS instrument was operated with the nebulizer at 60 psi, vaporizer at 400 °C, N_2 flow at 600 l/h, cone gas at 80 l/h, APCI source temperature at 95 °C, and APCI probe temperature at 550 °C. Selected ion monitoring (SIM) was used due to increase reproducibility and to reduce the signal/noise ratio (Schouten et al., 2007). SIM was set to scan $[M + H]^+$ of C_{46} GDGT (m/z 744), $[M + H]^+$ of crenarchaeol (m/z 1292) and $[M + H]^+$ of the brGDGTs (GDGT-I + GDGT-II + GDGT-III) (m/z 1050, 1036 and 1022), with a dwell time of 100 ms each. Quantification of GDGTs was obtained by comparing each respective $[M + H]^+$ peak area with that of the internal standard (Huguet et al., 2006), though this quantification does not matter for the BIT index. The average relative standard deviation (%) was < 10%. The BIT index can be used to estimate the relative contribution of branched and isoprenoidal GDGTs (Hopmans et al., 2004; Schouten et al., 2013a), defined as followed:

$$BIT = \frac{GDGT-\mathrm{I} + GDGT-\mathrm{II} + GDGT-\mathrm{III}}{GDGT-\mathrm{I} + GDGT-\mathrm{II} + GDGT-\mathrm{III} + Crenarchaeol} \quad (1)$$

4. Results

4.1. Sediment chronology and sediment grain size in cores

Fig. 2(a) and (b) present the $^{210}Pb_{ex}$ concentration profiles associated with the sediment cores collected from the subaqueous delta. The $^{210}Pb_{ex}$ activities varied from 0.11 to 5.20 dpm/g, with a mean of 1.86 dpm/g, respectively (Fig. 2(a) and (b)). $^{210}Pb_{ex}$ activities in downcore profiles were characterized by a progressive decline in activity with depth, reflecting sediment accumulation and the radioactive decay of the $^{210}Pb_{ex}$. Cesium-137 (^{137}Cs) is an artificial radionuclide with a half-life of 30 years. This radionuclide was released from thermonuclear weapons tests since 1952 and was spread globally. The frequent bomb testing across the globe contributed to a striking increase in the ^{137}Cs concentrations in the northern hemisphere after 1954, and the maximum ^{137}Cs global fallout occurred in 1963 (Everett et al., 2008). The ^{137}Cs activities in sediment cores YE-1 and DH-1 ranged from 0.01 to 0.33 ± 0.02 dpm/g, with an average of 0.13 ± 0.02 dpm/g (Fig. 2(c) and (d)). The ^{137}Cs peaks appear at depths of 108.5 cm and 76.5 cm depth in YE-1 and DH-1, respectively. The concentrations of $^{239+240}Pu$ in core YE-1 ranged from 0.072 ± 0.003 mBq/g to 0.02 ± 0.001 mBq/g, with an average of 0.215 ± 0.019 mBq/g (Fig. 2(c) and (d)). $^{239+240}Pu$ activities in core DH-1 varied between 0.03 ± 0.001 and 0.827 ± 0.09 mBq/g, with a mean of 0.230 ± 0.025 mBq/g (Fig. 2(c) and (d)). The peaks of $^{239+240}Pu$ activities appeared at 108.5 cm and 76.5 cm in core YE-1 and DH-1, in agreement with the peaks of ^{137}Cs in cores.

The maximum peaks of Pu and ^{137}Cs in cores YE-1 and DH-1, at the depths of 108.5 cm and 76.5 cm respectively, are attributed to the maximum radionuclide deposition in 1963 (Fig. 2c and d) (Everett et al., 2008). The sediment rates are 2.2 cm/yr and 1.3 cm/yr, calculated by the $^{239+240}Pu$ and ^{137}Cs data. Given the complex hydrodynamic environment in the estuary of Changjiang River and the inner shelf of ECS, and that cores are not long enough to reach the ^{210}Pb equilibrium point, the CRS (constant rate of supply) model may not be applicable in our study (Appleby, 2008; Guo and Yang, 2016). The Constant Initial Concentration (CIC) model was therefore used in this study and assumed that an increased flux of sedimentary particles from the water column will be deposited proportionally (Appleby, 2008). In recent years, the CIC model has been widely used in dating cores from the estuary and inner shelf of ECS (Ge et al., 2015; Meng et al., 2015; Gao et al., 2017; Guo and Yang, 2016; Zhao et al., 2016). Moreover, the mean sedimentation rates determined for cores YE-1 and DH-1 are 2.1 cm/yr and 1.4 cm/yr based on the CIC model, and are in good agreement with the results of the $^{239+240}Pu$ and ^{137}Cs data, covering a time span of 70 years and 116 years, respectively. The average errors of our age determinations in cores YE-1 and DH-1 are 1.8 yr and 1.3 yr, respectively (Fig. 2e). The observed pattern of sedimentation rates decreasing southward from estuary to offshore documented by these cores is similar to the results of a study in the adjacent area, which reported rates ranging from ~2 cm/yr to < 0.1 cm/yr (Huh and Su, 1999; Gao et al., 2017; Guo and Yang, 2016; Zhao et al., 2016).

The core YE-1 sediments consist mainly of yellow-gray and gray-black clayey silt. The relatively pure clay layer often contains intercalated silt. The profiles of mean grain size varied with depth in core YE-1 (Fig. 3a). The mean grain size had a range between 6.23Φ and 7.8Φ, with an average of 7.1Φ. The composition of clay and silt ranged from 16.23% to 35.8% and from 62.33% to 79.35%, with average values of 26.47% and 71.44%, respectively (Fig. 3a). However, the contents of sand in core YE-1 ranged 0–15.93%, with an average of 2.09%. In core DH-1, the yellow-gray clay dominates the whole of the facies, with occasional intercalating gray-black silt; shell fragments are occasional observed. The core DH-1 was dominated by silt (4Φ–8Φ) (> 70%) and clay (< 8Φ) (> 25%), with silt as the major component (Fig. 3b). The mean grain size in core DH-1varied in the range 6.6Φ–8.0Φ, with an average of 7.3Φ. The contents of silt (53.37–77.80%), clay (20.39–45.63%) averaged 70.96% and 28.41%, respectively. In contrast, sand contents are between 0 and 18.9% in core DH-1, with an average of 2.89%.

4.2. Sr-Nd isotopes and Zr/Rb in the core sediments from YE-1 and DH-1

The $^{87}Sr/^{86}Sr$ ratios in core YE-1 vary between 0.717783 and 0.725102, with an average of 0.721639, albeit with some fluctuations (Fig. 3 and Table S1). $^{143}Nd/^{144}Nd$ ratios vary from 0.511981 to 0.512112 (avg. 0.512033). εNd values range from −12.8 to −10.5,

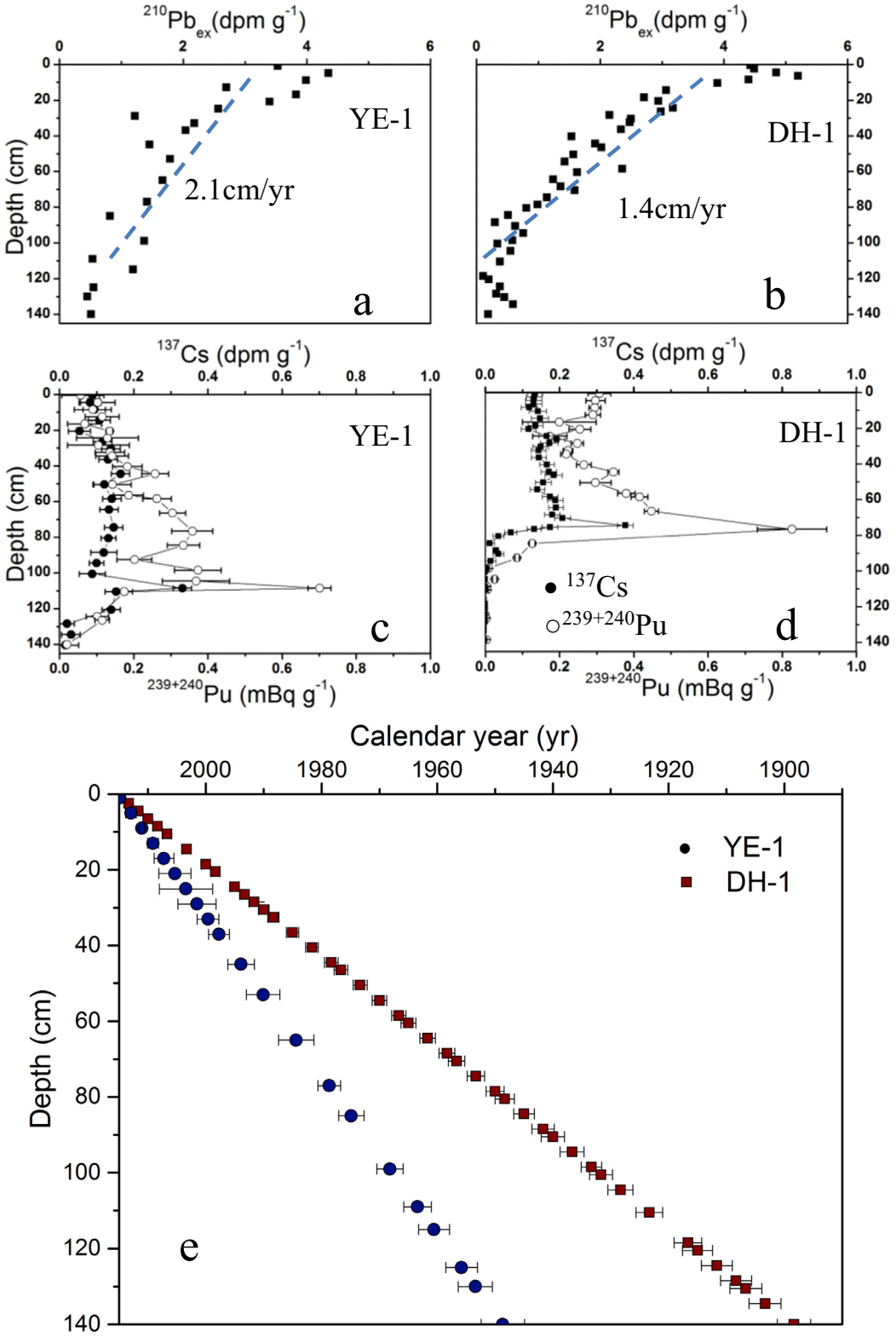

Fig. 2. Depth profiles of $^{210}Pb_{ex}$, ^{137}Cs and $^{239+240}Pu$ activities in core YE-1 and DH-1 of ECS. (a) $^{210}Pb_{ex}$ of core YE-1; (b) $^{210}Pb_{ex}$ of core DH-1 (c) ^{137}Cs and $^{239+240}Pu$ of core YE-1; (d) ^{137}Cs and $^{239+240}Pu$ of core DH-1, the error bars represent uncertainties based on the propagation of 1σ counting errors; (e) geochronology in cores.

with an average of −11.8 (Fig. 3 and Table S1). The average ratio of $^{87}Sr/^{86}Sr$ in core DH-1 is 0.723931 (range 0.720751–0.726489), and the average of εNd is −11.9 (range −12.7–11.1). $^{143}Nd/^{144}Nd$ ratios vary from 0.512069 to 0.511987 (avg. 0.512024). In addition, the average ratios of $^{87}Sr/^{86}Sr$ and $^{143}Nd/^{144}Nd$ in SSSs, collected from Xuliujing near the estuary, are 0.725099 (0.719351 to 0.731705) and 0.512015 (0.511940 to 0.512083), respectively, while εNd is −12.1 (−13.6 to −10.8) (Table. S1). In core YE-1, the Zr/Rb ratio varies between 1.04 and 2.02, with an average value of 1.46. The Zr/Rb ratio in core DH-1 varies from 0.91 to 1.80, with an average of 1.37.

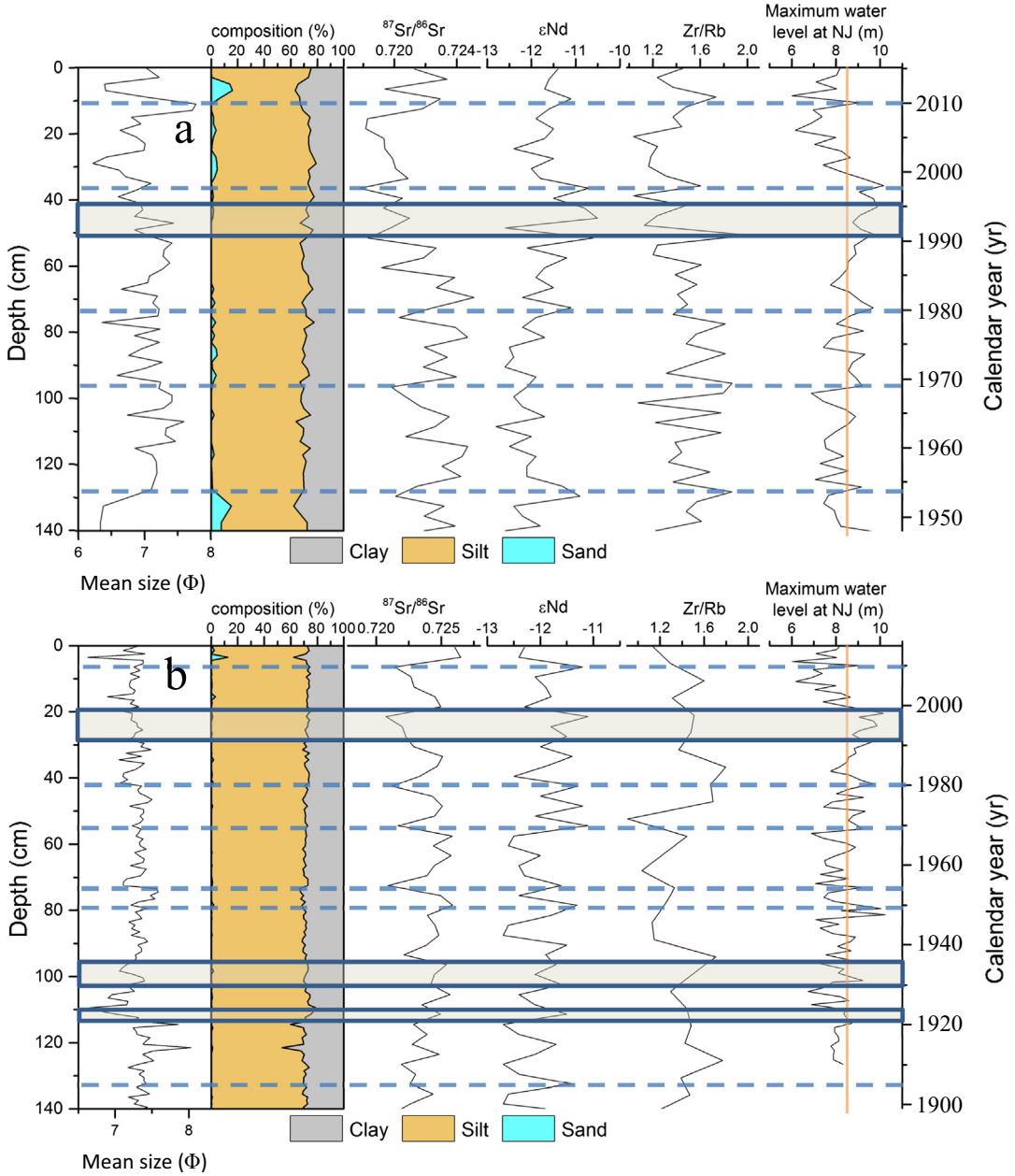

Fig. 3. Distributions of mean grain size (Mean size), sediment size proportion, Sr and Nd isotopes and Zr/Rb ratios cores YE-1 (a) and DH-1 (b) with the maximum water level at Nanjing hydrological gauge station (JPHWRIB, 2016). Dash lines mean extreme floods in 2010, 1998, 1980, 1969, 1954, 1949, 1905. Shadows mean extreme floods in 1991–1995/1998, 1931–1935, 1921–1922. Orange line (8.5 m) means the threshold of local flood occurrence at Nanjing.

4.3. TOC, brGDGTs, crenarchaeol and BIT index in sediment cores

The TOC contents of core samples are presented in Fig. 4 and range from 0.20 to 0.73%, with an average of 0.41%. TOC slightly increases from the bottom to top. BrGDGTs and crenarchaeol are detected in all core samples. The TOC normalized contents of brGDGTs for core YE-1 range from 21.9 to 32.8 ng/g TOC (avg. 26.2 ng/g TOC), while the concentrations of crenarchaeol range from 50.8 to 79.9 ng/g TOC. In core DH-1, brGDGTs varied between 17.7 and 30.9 ng/g TOC (avg. 22.5 ng/g TOC), crenarchaeol between 45.9 and 85.5 ng/g TOC (avg. 64.6 ng/g TOC). The BIT index varied from 0.16 to 0.28 in core YE-1, and from 0.13 to 0.3 in core DH-1. The sedimentary fluxes (SF) of the GDGTs varied from 45.5 to 78.9 ng/cm^2 yr in core YE-1 and 27.9 to 66.8 ng/cm^2 yr in core DH-1 for brGDGTs, and between 86.3 and 182.6 ng/cm^2 yr in core YE-1 and 96.5–195.3 ng/cm^2 yr in core DH-1 for crenarchaeol, respectively (Fig. 4).

5. Discussions

5.1. Sediment provenance in the estuary of the Changjiang River

Sr-Nd isotopic compositions of the sediments are useful to determine their provenance, if biogenic, organic, and authigenic components in the sediments and grain-size effect are fully eliminated. In this study, calcium carbonate, authigenic components, organic compounds, and biogenic silica should have been effectively removed, according to Sr-Nd isotopic compositions of only detrital components in the sediments (Bayon et al., 2002; Eggiman et al., 1980). Sr isotopic composition is overall not influenced by separation and formation of chemical phases, and evaporation and biologic assimilation (Goldstein and Jacobsen, 1988). Sediment grain size may influence Sr isotope ratios of detrital materials due to varying mineralogy, and hence isotopic compositions of fractions of different sizes. Fine-grained fractions tend to be

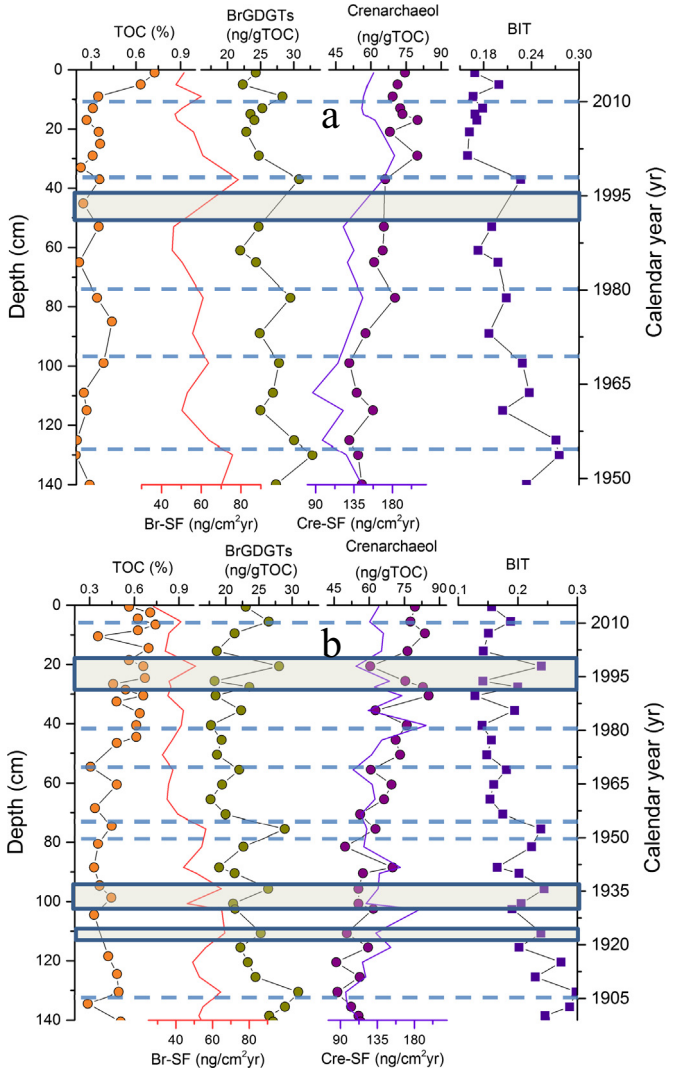

Fig. 4. Vertical profiles of TOC contents, TOC normalized contents of brGDGTs and crenarchaeol, sedimentary fluxes of brGDGTs (Br-SF) and crenarchaeol (Cre-SF) and BIT index in core sediments from the subaqueous delta of Changjiang River. (a) core YE-1; (b) core DH-1. Dash lines mean extreme floods in 2010, 1998, 1980, 1969, 1954, 1949, 1905. Shadows mean extreme floods in 1991–1995/1998, 1931–1935, 1921–1922.

enriched in radiogenic ^{87}Sr because of high Rb/Sr ratios in micas in general and biotite in particular (Dasch, 1969; Feng et al., 2009). In contrast, Nd isotope behaves conservatively, and the size fractions from the same source have similar εNd values (Goldstein and Jacobsen, 1988; Borg and Banner, 1996; Jiang et al., 2013). Grain size variation in our cores is not large (6.2 to 7.8Φ in mean grain size), and grain size does not change significantly through the cores (Fig. 3a and b). Accordingly, $^{87}Sr/^{86}Sr$ ratios show no significant correlations with grain size in the core sediments of YE-1 and DH-1 (r = 0.03 and 0.14, respectively; Fig. 3a and b). Nd isotopic ratios in core YE-1 and DH-1 are also not correlated with grain size (Fig. 3a and b). The poor correlations among mean grain size, Sr-Nd isotopic compositions (Fig. 3a and b) suggest that the grain-size effect may not be an important cause of vertical changes of Sr-Nd isotopic compositions in the cores.

As discussed above, the Sr-Nd isotopes of the sediments in ECS mainly reflect the complex controls of provenance rocks and chemical weathering between different tributary catchments (Yang et al., 2007, 2015b; Luo et al., 2012; Li et al., 2015a; He et al., 2015; Bi et al., 2017). Analysis of the isotopic data from core samples of YE-1 and DH-1 as well as potential river sources and other regions using a discrimination

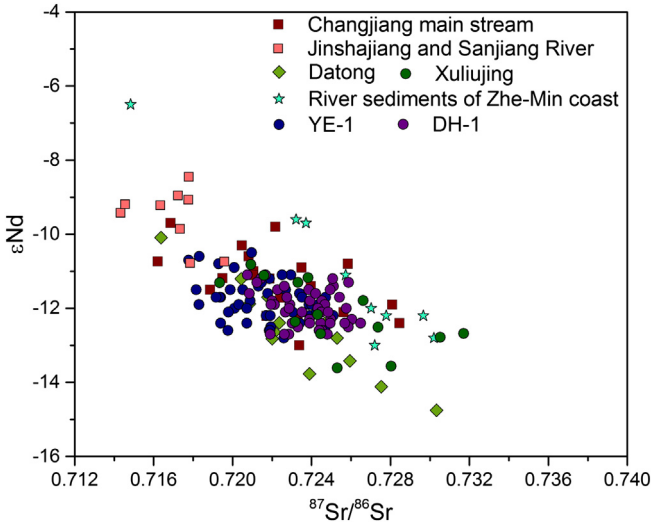

Fig. 5. Discrimination diagrams of εNd versus $^{87}Sr/^{86}Sr$ in Core YE-1 and DH-1 sediments, in comparison with those of potential river sources. Isotope data of potential provenances including the Changjiang main stream (Yang et al., 2007; He et al., 2015), Sanjiang and Jinshajiang River (Wu et al., 2010), small river sediments of Zhe-Min coast (Bi et al., 2017), SSSs from Datong hydrological gauging station (Luo et al., 2012) and Xuliujing hydrological gauge station. Jinshajiang River is at the upper part of Changjiang River, Sanjiang River is at the origin of Changjiang River, Datong hydrological gauging station is the boundary between the middle and lower catchment of Changjiang River, and Xuliujing is the origination of the estuary.

diagram of $^{87}Sr/^{86}Sr$ vs. εNd (Fig. 5) indicates that the upper reaches of the Changjiang River are characterized by high εNd values and low $^{87}Sr/^{86}Sr$ ratios, highlighted by the Jinshajiang River at the upper part of Changjiang River and Sanjiang River at the origin of Changjiang River (Fig. 5, Yang et al., 2007; He et al., 2015). In contrast, sediments of the mid-lower mainstream display high $^{87}Sr/^{86}Sr$ ratios and low εNd values (Fig. 5, Yang et al., 2007; He et al., 2015). The small rivers in the Zhe-Min regions have relatively higher εNd values and $^{87}Sr/^{86}Sr$ ratios (Fig. 5, Bi et al., 2017). These are remarkably different from those of the YE-1 and DH-1 samples and the modern Changjiang sediment as well. No obvious difference exists in Sr-Nd isotopic compositions between the core samples and the modern Changjiang sediment samples (Fig. 5). In addition, variations of Sr-Nd isotopic composition in core sediments are similar to those of the suspended sediments at Xuliujing near the Changjiang River estuary. Together these data indicate that the core sediments of both YE-1 and DH-1 are predominantly sourced from the Changjiang, and are not significantly affected by other small rivers.

5.2. Identification and reconstruction of flooding events based on Sr-Nd isotopic signatures and Zr/Rb

$^{87}Sr/^{86}Sr$ ratios and εNd show obvious fluctuations in core YE-1 and DH-1 (Fig. 3). $^{87}Sr/^{86}Sr$ minima occur in 2010, 1993–1998, 1980, 1954, 1949, 1936, 1923, 1898 in core YE-1 and DH-1. In contrast, these years are characterized by high εNd values. These variations in Sr-Nd isotopic signatures correspond to times of high water levels at Nanjing hydrological gauge station during the last century (JPHWRIB, 2016) (Fig. 3). Moreover, Sr-Nd isotopic signatures of SSSs from Xuliujing display distinct seasonal variations, with minimum $^{87}Sr/^{86}Sr$ ratios and maximum εNd values during the flood season (July to September) (Table S1). Our SSSs in Xuliujing span a large hydrological gradient of the Changjiang River, especially containing large floods in 2016. In 2016, this flood from June 30 to July 7 is the third largest flood after floods of 1998 and 1954, and the peak water level is over 9.96 m at Nanjing (JPHWRIB, 2016). The SSSs at Xuliujing during the large flood in 2016 have lower $^{87}Sr/^{86}Sr$ ratios and higher εNd values during the flood

season than the dry season (Table S1), which is consistent with previous studies (Mao et al., 2011; Luo et al., 2012). Although all SSSs are collected from the middle level of Xuliujing, where the isotopic composition of SSSs can represent that of the material transported by the Changjiang River (Luo et al., 2012), other small rivers can deliver regional sediments into the hydrological section at Xuliujing, leading to slight differences between our results and previous studies (Mao et al., 2011; Luo et al., 2012).

These seasonal variations primarily reflect the controls of provenance rocks and erosion in different sub-catchments. According to previous studies, the upper catchment of the Changjiang River plays an important role in this process because it supplies most of the suspended sediments to the ocean (Zhang, 1999; Chen et al., 2002; Chen et al., 2001). During flood season, heavy precipitation shifts toward the upper catchment, while middle-lower catchment receives little precipitation due to the influence of the subtropical high (CWRC, 2002; Huang et al., 2007; Gu, 2015). The results suggest that strengthened physical erosion of source rocks in the upper catchments during such periods leads to an increased contribution of sediment loads (CWRC, 2014; CWRC, 2015). In addition, the contributions of sediment loads from the upper catchment are up to 80% at Yichang gauge station in flood (CWRC, 2015). Considering the weaker physical erosion and channel erosion in the middle-lower catchments, relatively little local sediment may contribute to the sediment load of the Changjiang River, with radiogenic Sr and non-radiogenic Nd (Mao et al., 2010). In contrast, due to heavy precipitations from the EASM and ISM (Gu, 2015), suspended sediments from the upper catchments dominate the sediment loads of the Changjiang River, with the higher εNd values and the lower $^{87}Sr/^{86}Sr$ ratios from upstream transported into the lower Changjiang River (Mao et al., 2011; Luo et al., 2012). Therefore, the extreme peaks of Sr and Nd isotopic compositions are correlated with historical flooding events in the upper catchment of the Changjiang River (e.g. 2010, 1993–1998, 1980, 1954, 1949, 1935–1936, 1921–1922, 1896–1898) (Shi et al., 2004; Wang et al., 2011; Hu et al., 2014).

Previous research indicated that variations in grain size of flood event deposits can be used to identify single flood event layers (Middelkoop et al., 2010; Toonen et al., 2012). Other studies have correlated flood event layers with historical flood events by making use of historical records (Aloserij, 2013; Toonen, 2013). However, given the complex catchment configuration and considerable mixing of sediments, it may be complicated for traditional fingerprinting of paleo-floods based on sediment grain size information (Ypma, 2014). It is more reliable that the chemical composition (e.g. Zr/Rb) of a sedimentary sequence may be used to identify flood deposits and to trace flood events (Walling, 2005; Macklin et al., 2006; Kylander et al., 2011; Heinecke et al., 2016). For instance, the main source of Zirconium (Zr) is the heavy mineral Zircon, which is released by physical rather than chemical weathering and associated with coarse silt and sand fractions (Chen et al., 2006; Kylander et al., 2011; Heinecke et al., 2016). Rb is present in several common minerals including mica and clay minerals (Kalugin et al., 2007; Kylander et al., 2011; Wang et al., 2011). During chemical weathering, Rb tends to be enriched in clay minerals. Thus, Zr/Rb ratio often reflects the content of coarse minerals relative to clay minerals, and is often used as a paleo-flood proxy in Quaternary research (Liu et al., 2006; Heinecke et al., 2016).

The acceleration of the river flow velocity will transport a large quantity of coarse sediment during floods (Wang et al., 2011; Hu et al., 2014; Zhao et al., 2016). This results in an increase in the coarse content relative to the fine particles within the delta, with higher Zr/Rb ratio (Wang et al., 2011; Hu et al., 2014). In core YE-1, the Zr/Rb ratio ranges between 1.04 and 2.02, with an average of 1.46 (Fig. 3a). In core DH-1, the Zr/Rb ratio varies from 0.91 to 1.80, with an average of 1.37 (Fig. 3b). Some peaks of Zr/Rb occur in 2010, 1993–1998, 1991, 1955, 1938, 1923 and 1899 CE in core YE-1 and DH-1, which are correlated to floods in the Changjiang River. Other peaks of Zr/Rb are also found in non-flood sedimentary facies. It may be suggested that a stronger winter monsoon can prefer to carry coarse dust to input to the marginal sea (Liu et al., 2004). As mentioned above, these data indicate severe floods in our sedimentary sequence can be identified by multiple sediment proxies (Fig. 3). However, Sr-Nd isotopic signatures and Zr/Rb ratio seem relatively invariant during the historical floods. It is indicated that some flood deposits may be missed in sediment records, for example, the floods of 1949 and 1923. Obviously, relatively large flood events may be recorded in subaqueous delta; thus the missing evidence of small-scale floods could be attributed to sediment reworking. Alternative explanation is that low-resolution age control as well as strong currents in coastal areas of the ECS may limit the identification of high-resolution flood events. Further, it is needed to consider the reliability of Sr-Nd isotopic proxy to reconstruct the paleo-flood records in the coastal area.

5.3. Distributions of brGDGTs, crenarchaeol and BIT in cores and applicability to reconstructing historical floods

BrGDGTs concentrations, fluxes, and the BIT index in core YE-1 sediments are higher than in core DH-1 sediments, whereas, the contents and sediment fluxes of crenarchaeol are slightly higher in DH-1 than in YE-1 (Fig. 4(a) and (b)). This may be ascribed to differences in the relative locations of these cores within the estuary. Core YE-1 was closer to the estuary than core DH-1, which was near the front of the subaqueous delta. BrGDGTs were closely associated with river and soil materials from the Changjiang River. Therefore, these terrigenous materials are preferentially deposited in core YE-1, resulting in relatively abundant brGDGTs. However, highly turbidity and low water transparency in the estuary might be unfavourable for marine production (Zhu et al., 2011; Kim et al., 2014; Lv et al., 2014, 2015). As a result, low crenarchaeol in sediment might be accumulated at core YE-1 (avg. 62.3 ng/g) than DH-1 (avg. 64.6 ng/g). That said, it is noteworthy that recent studies have revealed that brGDGTs transported by rivers are not necessarily exclusively derived from the surrounding soils, but may also be produced in situ (Tierney and Russell, 2009; Zhu et al., 2011; Kim et al., 2014; Yang et al., 2013; Zell et al., 2013; De Jonge et al., 2014; Lv et al., 2014; Li et al., 2015b; Zhou et al., 2014). In addition, some studies reported that crenarchaeol may be distributed in soils (Weijers et al., 2006; Li et al., 2017). However, the impact of such origins is almost certainly dependent on the depositional setting, and is of minor importance in the sections of the Changjiang studied so far (Zhu et al., 2011; Yang et al., 2013; Li et al., 2015b). As a result, brGDGTs and the BIT index are still hypothesized to track the input of continental OC and thus may serve as a palaeoflood proxy (Zhu et al., 2011; Kim et al., 2014; Yang et al., 2013; Lv et al., 2014).

In core YE-1 and DH-1, crenarchaeol concentrations and sedimentary fluxes show a gradual increasing trend during the last century (Fig. 4(a) and (b)). In contrast, the profiles of brGDGT contents, brGDGT fluxes and BIT gradually decrease in the last decades, coinciding with a reduction in annual sediment discharges from the Changjiang River (Yang et al., 2014, 2015a; Dai and Lu, 2014; Dai et al., 2016). In addition, TOC contents increase in both cores (Fig. 4(a) and (b)). In the past decades, anthropogenic activities (e.g., dam constructions and soil conservations) in the drainage basin of Changjiang River result in the decline of terrestrial sediment inputs, which may explain the decline of brGDGTs and decrease of BIT in the subaqueous delta. However, fertilizer usages, reclamation and agricultural plantations in the drainage basin, changes of land cover and vegetation type, could discharge more terrigenous organic materials into the ECS (Chen et al., 2017), leading to the increase of TOC in sediment cores. Additionally, nutrient input derived from anthropogenic sources could enhance marine productivity, which would explain the increasing trends in crenarchaeol profiles.

Previous research showed that the concentration of brGDGTs increased from the upper reaches toward the lower reaches of the Changjiang, with a range of 0.1 to 7.6 μg/g (Li et al., 2015b). In

addition, values for the BIT index in Changjiang River catchment ranged from 0.70 to 0.91, with an average of 0.85 (Li et al., 2015b; Zhu et al., 2011; Lv et al., 2015). In the estuary of Changjiang River and continental shelf of ECS, variation in the concentration of brGDGTs is closely related to sediment discharge from the Changjiang River, with a substantially higher BIT value (> 0.8) in the Lower Changjiang River than that for the offshore surface sediment (< 0.04) (Zhu et al., 2011; Lv et al., 2015). It is therefore reasonable that the BIT index, in conjunction with brGDGTs and crenarchaeol concentrations, might be applied as a proxy to identify and reconstruct flooding events in the subaqueous delta of Changjiang River. Higher values of br GDGTs and BIT and lower crenarchaeol occur in 2010, 1993–1998, 1980, 1954, 1949, 1936, 1920, 1909 and 1897 (Fig. 4(a) and (b)). These events generally correlate with historically documented floods on the Changjiang River (e.g., 2010, 1998, 1995, 1993, 1980, 1954, 1949, 1936, 1920, 1909 and 1896–1898) (Shi et al., 2004; Wang et al., 2011; Hu et al., 2014). In the flooding extremes, strong river currents could transport soil materials from the Changjiang River catchment, and cause high turbidity and low transparency in the estuary. In contrast, a location far from the estuary such as core DH-1 will not receive abundant catchment particulate materials, but could receive enhanced riverine nutrient to stimulate marine primary productivity. This could indirectly increase the abundance of crenarchaeol, resulting in a decrease in brGDGTs and the BIT index. This probably explains the variations of brGDGT concentrations and the BIT index, as well as crenarchaeol concentration in sedimentary records of the subaqueous delta (Fig. 4(a) and (b)). Hence, these high values of brGDGT and the BIT index as well as low crenarchaeol could be considered as a paleoflooding proxy in sedimentary sequence, which closely corresponded to floods events of the Changjiang River.

5.4. Linkages between extreme events and global climate changes

The Sr-Nd isotopes and biomarker can be used to trace and reconstruct the flood events in the Changjiang River catchment. The relationships of the geochemical proxies of flood events (e.g. Sr-Nd isotopes, Zr/Rb and biomarker) and historical records (e.g. peak water level) elucidate the response of sedimentary processes of the subaqueous delta in Changjiang River to paleoclimate changes, because the physical processes represented by these proxies and the maximum water level are different. The geochemical proxies are mainly associated with changes of terrigenous inputs, and are indirectly impacted by atmospheric system, whereas the maximum water level is mainly controlled by climate changes. Cross spectral analysis could be performed between the record of the geochemical proxies and the maximum water level in Nanjing hydrological gauge station (JPHWRIB, 2016) to compare their variation paces. Cross spectral analysis is often used to estimate the relation-ship between two time series as a function of frequency (Paillard et al., 1996; Schulz and Stattegger, 1997; Cronin et al., 2002; Quinn et al., 2006; Wei et al., 2009; Olafsdottir et al., 2016). Fig. 6 shows the cross spectra between the maximum water level records and the Sr-Nd isotopes, Zr/Rb, and biomarker in core DH-1, which spans over a hundred years. The results reveal a coherent relationship between Sr-Nd isotopes and the maximum water level at periods of 14.3, 6.5 and 3.2 yr, with Sr-Nd isotopes lagging floods by 1.8 mo. Coherent relationships of Zr/Rb and the maximum water level are also evident at 14, 6.5 and 3.5 yr, respectively, with Zr/Rb ratio lagging the maximum water level by 2.1 mo (Fig. 6c). In addition, the cross spectrum of BIT and the maximum water level records reveal coherences center at 13 yr and 3 yr, with BIT lagging the maximum water level by 2.5 mo (Fig. 6d). This suggests a link between major floods in the Changjiang River and atmosphere-oceanic circulation patterns, especially El Nino Southern Oscillation (ENSO) events (Xu et al., 2005; Wu et al., 2005; Jiang et al., 2008; Xiao et al., 2015).

Indeed, ENSO is the leading driver of seasonal precipitation variability over the Changjiang River basin (Xu et al., 2005; Wu et al., 2005; Jiang et al., 2008; Xiao et al., 2015). ENSO variance can cause widespread flooding and create hazardous storms in eastern China (Yu et al., 2009; Huang et al., 2007). ENSO has significant periodicities ranging from 3 to 8 yr (Wu et al., 2005; Jiang et al., 2008; Xiao et al., 2015). The 3–6.5 yr patterns of geochemical data in core DH-1 are reminiscent of ENSO related anomalies in observational data. Thus, floods originating from the Changjiang River mainly correspond to ENSO circulation. In addition, the other significant periodicity in our geochemical data centers at 13–14.2 yr in the subaqueous delta (Fig. 6). Recent studies reported that the discharge of the Changjiang River has periods of over 10 years (Zhang et al., 2006). It is suggested that the flooding events on the eastern China can be impacted by other long-term atmosphere-oceanic circulation patterns, for example, Pacific Decadal Oscillation (PDO), which is centered on periodicities of > 10 yr (Yu et al., 2009; Huang et al., 2007). Therefore, the multi-proxy approach (Sr-Nd isotopic signatures, Zr/Rb ratio, brGDGTs and the BIT index) in the subaqueous delta of Changjiang River can be used to trace the climate changes occurring to sediment sequences. As a whole, although having their own drawbacks or limitations, these proxies seem to be feasible to unravel the complete story with many processes occurring in the marginal sea, based on geochemical tools and biomarker records. With a view to applying sediment source indicators, their applicability should be carefully evaluated, especially the different sources between unique isotopic signals and biomarkers. More efforts are still needed to evaluate the effect of diverse original sources on the relevant proxies, trying to further understand such complex sedimentary environments.

6. Conclusions

Subaqueous delta sediments of the Changjiang River can be used to reconstruct flooding events, based on sedimentary Sr-Nd isotopic signatures, Zr/Rb ratios, and biomarkers (e.g., brGDGTs and the BIT index as well as crenarchaeol), illustrating complex responses to flooding events during the last century. The variabilities of low $^{87}Sr/^{86}Sr$ ratios, high εNd values and Zr/Rb ratio can correspond to the frequencies of historical floods in the Changjiang River. Comparison of these data to extreme floods of the Changjiang River confirms that these proxies record floods in these our cores. In addition, although there were some complications in terms of the applications of biomarkers (e.g., brGDGTs, the BIT index as well as crenarchaeol) as a palaeoflood proxy, variations of these biomarkers were corresponded to historical floods events of the Changjiang River. The results showed that the BIT index, combined with brGDGTs and crenarchaeol concentrations, could provide a potential method to trace and reconstruct the palaeoflood events in the estuary. Based on cross-spectral analyses of the Sr-Nd isotopic compositions and maximum water levels in Nanjing, floods exhibited a 3–6 yr cyclicity, showing that floods in the Changjiang River may be impacted by ENSO variability. At the same time, the variability of Sr-Nd isotopic signatures also occur on > 10 yr, implying that the historical floods may be controlled by the long-term decadal cycle.

Supplementary data to this article can be found online at https://doi.org/10.1016/j.chemgeo.2018.09.003.

Acknowledgments

This work was financed by the National Natural Science Foundation of China (41406055, 41506106), the Strategic Priority Research Program of the Chinese Academy of Sciences (XDA11030104), the project of Global Change and Air-Sea Interaction, International Postdoctoral Exchange Fellowship Program (20160073), Natural Science Foundation of Jiangsu Province (BK20170451, BE2016701), Six talent peaks project in Jiangsu Province (JNHB-143), Natural Science Foundation of Lianyungang City (SH1506, CN1510). We are also grateful to “Qing Lan Project” of Jiangsu Provincial Department of Education and the Priority Academic Program Development of Jiangsu Higher Education Institutions.

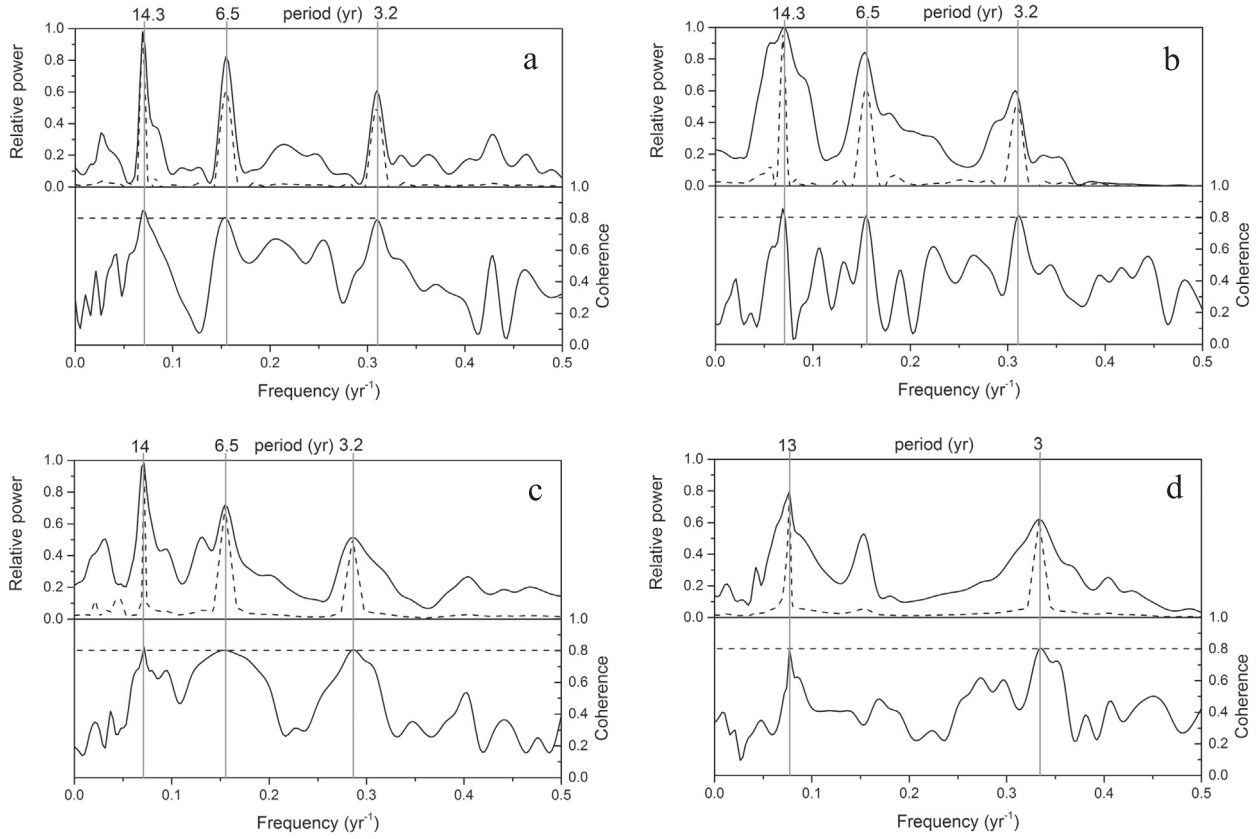

Fig. 6. Cross-spectral analyses on the $^{87}Sr/^{86}Sr$ ratios and εNd with the maximum water level of Nanjing hydrological gauging station during the last century. (a) $^{87}Sr/^{86}Sr$ ratios, (b) εNd, (c) Zr/Rb, (d) BIT.

References

Aloserij, L.H.J., 2013. Historical Floods of the Rhine River, Reconstructed from the Sedimentary Fills of a Dike Breach Pond and Abandoned Channels: Application for Recalculation of the Design Discharge. Utrecht University, Utrecht (Master Thesis).

Appleby, P.G., 2008. Three decades of dating recent sediments by fallout radionuclides: a review. The Holocene 18, 83–93.

Bayon, G., German, C.R., Boella, R.M., Milton, J.A., Taylor, R.N., Nesbitt, R.W., 2002. An improved method for extracting marine sediment fractions and its application to Sr and Nd isotopic analysis. Chem. Geol. 187, 179–199.

Bi, L., Yang, S., Zhao, Y., Wang, Z., Dou, Y., Li, C., Zheng, H.B., 2017. Provenance study of the Holocene sediments in the Changjiang (Yangtze River) estuary and inner shelf of the East China Sea. Quat. Int. 441, 147–161.

Borg, L.E., Banner, J.L., 1996. Neodymium and strontium isotopic constraints on soil sources in Barbados, West Indies. Geochim. Cosmochim. Acta 60 (21), 4193–4206.

Cai, S.M., Du, Y., Huang, J.L., Wu, S.J., Xue, H.P., 2001. Causes of flooding and water logging in middle reaches of The Yangtze River and construction of decision-making support system for monitoring and evaluation of flooding and water logging hazards. Earth Sci. 26, 643–647 (In Chinese).

Changjiang Water Resource Commission (Ministry of Water Resources, China) (CWRC), 2002. Floods and Droughts in the Yangtze River Catchment. Water Conservancy and Water Electricity Publication House, Beijing.

Changjiang Water Resource Commission (Ministry of Water Resources, China) (CWRC), 2015. Bulletin of Yangtze River Sediment. Press of Ministry of Water Resources of China, Beijing (in Chinese).

Changjiang Water Resources Commission (Ministry of Water Resources, China) (CWRC), 2014. Hydrological Records of the Yangtze River. Cyclopaedia Press of China, Beijing (in Chinese).

Chen, Z., Li, J., Shen, H., Wang, Z.H., 2001. Yangtze River of China: historical analysis of discharge variability and sediment flux. Geomorphology 41, 77–91.

Chen, J.S., Wang, F.Y., Xia, X.H., 2002. Major element chemistry of the Changjiang (Yangtze River). Chem. Geol. 187, 231–255.

Chen, J., Chen, Y., Liu, L., Ji, J., Balsam, W., Sun, Y., Lu, H., 2006. Zr/Rb ratio in the Chinese loess sequences and its implication for changes in the East Asian winter monsoon strength. Geochim. Cosmochim. Acta 70 (6), 1471–1482.

Chen, J., Li, G.J., Yang, J.D., Rao, W.B., Lu, H.Y., Balsam, W., Sun, Y.B., Ji, J.F., 2007. Nd and Sr isotopic characteristics of Chinese deserts: implications for the provenances of Asian dust. Geochim. Cosmochim. Acta 71, 3904–3914.

Chen, L., Liu, J., Xing, L., Krauss, K.W., Wang, J., Xu, G., Li, L., 2017. Historical changes in organic matter input to the muddy sediments along the Zhejiang-Fujian Coast, China over the past 160 years. Org. Geochem. 111, 13–25.

Cronin, T.M., Dwyer, G.S., Schwede, S.B., Vann, C.D., Dowsett, H., 2002. Climate variability from Florida Bay sedimentary record: possible teleconnections to ENSO, PNA and CNP. Clim. Res. 19, 233–245.

Dai, S.B., Lu, X.X., 2014. Sediment load change in the Yangtze River (Changjiang): a review. Geomorphology 215, 60–73.

Dai, Z., Fagherazzi, S., Mei, X., Gao, J., 2016. Decline in suspended sediment concentration delivered by the Changjiang (Yangtze) River into the East China Sea between 1956 and 2013. Geomorphology 268, 123–132.

Dasch, E.J., 1969. Strontium isotopes in weathering profiles, deep-sea sediments, and sedimentary rocks. Geochim. Cosmochim. Acta 33, 1521–1552.

De Jonge, C., Stadnitskaia, A., Hopmans, E.C., Cherkashov, G., Fedotov, A., Sinninghe Damsté, J.S., 2014. In situ produced branched glycerol dialkyl glycerol tetraethers in suspended particulate matter from the Yenisei River, Eastern Siberia. Geochim. Cosmochim. Acta 125, 476–491.

DeMaster, D.J., McKee, B.A., Nittrouer, C.A., Jiangchu, Q., Guodong, C., 1985. Rates of sediment accumulation and particle reworking based on radiochemical measurements from continental shelf deposits in the East China Sea. Cont. Shelf Res. 4, 143–158.

Eggiman, D.W., Manheim, F.T., Betzer, P.R., 1980. Dissolution and analysis of amorphous silica in marine sediments. J. Sediment. Petrol. 50, 215–225.

Everett, S.E., Tims, S.G., Hancock, G.J., Bartley, R., Fifield, L.K., 2008. Comparison of Pu and ^{137}Cs as tracers of soil and sediment transport in a terrestrial environment. J. Environ. Radioact. 99, 383–393.

Feng, J.L., Zhu, L.P., Zhen, X.L., Hu, Z.G., 2009. Grain size effect on Sr and Nd isotopic compositions in eolian dust: implications for tracing dust provenance and Nd model age. Geochem. J. 43, 123–131.

Gao, S., Wang, D., Yang, Y., Zhou, L., Zhao, Y., Gao, W., Han, Z., Yu, Q., Li, G., 2016. Holocene sedimentary systems on a broad continental shelf with abundant river input: process-product relationships. Geol. Soc. Lond., Spec. Publ. 429, 223–259.

Gao, J.H., Jia, J., Sheng, H., Yu, R., Li, G.C., Wang, Y.P., Yang, Y., Zhao, Y., Li, J., Bai, F., Xie, W., Wang, A., Zou, X., Gao, S., 2017. Variations in the transport, distribution, and budget of ^{210}Pb in sediment over the estuarine and inner shelf areas of the East China Sea due to Changjiang catchment changes. J. Geophys. Res. Earth Surf. 122. https://doi.org/10.1002/2016JF004130.

Ge, H., Zhang, C.L., Li, J., Versteegh, G.J., Hu, B., Zhao, J., Dong, L., 2014. Tetraether lipids from the southern Yellow Sea of China: implications for the variability of East Asia Winter Monsoon in the Holocene. Org. Geochem. 70, 10–19.

Ge, C., Zhang, W., Dong, C., Dong, Y., Bai, X., Liu, J., Hien, N.T.H., Feng, H., Yu, L., 2015. Magnetic mineral diagenesis in the river-dominated inner shelf of the East China Sea, China. J. Geophys. Res. Solid Earth 120, 4720–4733.

Goldstein, S.J., Jacobsen, S.B., 1988. Nd and Sr isotopic systematics of river water suspended material: implications for crustal evolution. Earth Planet. Sci. Lett. 87,

249–265.
Grousset, F., Biscaye, P., 2005. Tracing dust sources and transport patterns using Sr, Nd and Pb isotopes. Chem. Geol. 222, 149–167.
Gu, H.M., 2015. Studyon Precipitation Characteristics and iTs Relationship With the Flood in the Yangtze River Catchment. Nanjing University of Information Science & Technology, Nanjing (Doctoral dissertation).
Guo, Y.W., Yang, S.Y., 2016. Heavy metal enrichments in the Changjiang (Yangtze River) catchment and on the inner shelf of the East China Sea over the last 150 years. Sci. Total Environ. 543, 105–115.
Guo, Z., Lin, T., Zhang, G., Zheng, M., Zhang, Z., Hao, Y., Fang, M., 2007. The sedimentary fluxes of polycyclic aromatic hydrocarbons in the Yangtze River Estuary coastal sea for the past century. Sci. Total Environ. 386, 33–41.
He, M., Zheng, H., Clift, P.D., Tada, R., Wu, W., Luo, C., 2015. Geochemistry of fine-grained sediments in the Yangtze River and the implications for provenance and chemical weathering in East Asia. Prog Earth Planet Sci. 2, 1–20.
Heinecke, L., Mischke, S., Adler, K., Barth, A., Biskaborn, B.K., Plessen, B., 2016. Late Pleistocene to Holocene climate and limnological changes at Lake Karakul (Pamir Mountains, Tajikistan). Clim. Past 1-30.
Hopmans, E.C., Weijers, J.W.H., Schefuß, E., Herfort, L., Sinninghe Damsté, J.S., Schouten, S., 2004. A novel proxy for terrestrial organic matter in sediments based on branched and isoprenoid tetraether lipids. Earth Planet Sc. Lett. 224, 107–116.
Hu, G., Li, A., Liu, J., Xu, G., Mei, X., Kong, X., 2014. High resolution records of flood deposition in the mud area off the Changjiang River mouth during the past century. Chin. J. Oceanol. Limnol. 32, 909–920.
Huang, R., Chen, J., Huang, G., 2007. Characteristics and variations of the East Asian monsoon system and its impacts on climate disasters in China. Adv. Atmos. Sci. 24, 993–1023 (in Chinese with English abstract).
Huguet, C., Hopmans, E.C., Febo-Ayala, W., Thompson, D.H., Sinninghe Damsté, J.S., Schouten, S., 2006. An improved method to determine the absolute abundance of glycerol dibiphytanyl glycerol tetraether lipids. Org. Geochem. 37, 1036–1041.
Huguet, C., Smittenberg, R.H., Boer, W., Sinninghe Damsté, J.S., Schouten, S., 2007. Twentieth century proxy records of temperature and soil organic matter input in the Drammensfjord, southern Norway. Org. Geochem. 38, 1838–1849.
Huh, C.A., Su, C.C., 1999. Sedimentation dynamics in the East China Sea elucidated from ^{210}Pb, ^{137}Cs and ^{239,240}Pu. Mar. Geol. 160, 183–196.
Jacobsen, S.B., Wasserburg, G.J., 1980. Sr-Nd isotopic evolution of chondrites. Earth Planet. Sci. Lett. 50, 139–155.
Jiang, T., Su, B., Hartmann, H., 2007. Temporal and spatial trends of precipitation and river flow in the Yangtze River Basin. Geomorphology 85, 143–154.
Jiang, T., Kundzewicz, Z.W., Su, B., 2008. Changes in monthly precipitation and flood hazard in the Yangtze River Basin, China. Int. J. Clim. 28, 1471–1481.
Jiang, F.Q., Frank, M., Li, T.G., Chen, T.Y., Xu, Z.K., Li, A.C., 2013. Asian dust input in the western Philippine Sea: evidence from radiogenic Sr and Nd isotopes. Geochem. Geophys. Geosyst. 14, 1538–1551.
Jiangsu Province Hydrology and Water Resources Investigation Bureau (JPHWRIB), 2016. Hydrology Statistics of Jiangsu Province. Jiangsu Province Hydrology and Water Resources Investigation Bureau, Nanjing.
Kalugin, I., Daryin, A., Smolyaninova, L., Andreev, A., Diekmann, B., Khlystov, O., 2007. 800-yr-long records of annual air temperature and precipitation over southern Siberia inferred from Teletskoye Lake sediments. Quat. Res. 67 (3), 400–410.
Kim, J.H., Buscail, R., Bourrin, F., Palanques, A., Sinninghe Damsté, J.S., Bonnin, J., Schouten, S., 2009. Transport and depositional process of soil organic matter during wet and dry storms on the Têt inner shelf (NW Mediterranean). Palaeogeogr. Palaeoclimatol. Palaeoecol. 273, 228–238.
Kim, J.H., Buscail, R., Fanget, A.S., Eyrolle-Boyer, F., Bassetti, M.A., Dorhout, D., Baas, M., Berné, S., Sinninghe Damsté, J., 2014. Impact of river channel shifts on tetraether lipids in the Rhône prodelta (NW Mediterranean): Implication for the BIT index as an indicator of palaeoflood events. Org. Geochem. 75, 99–108.
Kylander, M.E., Ampel, L., Wohlfarth, B., Veres, D., 2011. High-resolution X-ray fluorescence core scanning analysis of Les Echets (France) sedimentary sequence: new insights from chemical proxies. J. Quat. Sci. 26 (1), 109–117.
Li, C.A., Zhang, Y.F., 2004. Flood sedimental characteristic and its mark on the middle reaches of Yangtze River. Adv. Water Sci. 15, 485–488 (in Chinese with English abstract).
Li, T.G., Xu, Z.K., Lim, D., Chang, F.M., Wan, S.M., Jung, H.S., Choi, et al., 2015a. Sr-Nd isotopic constraints on detrital sediment provenance and paleoenvironmental change in the northern Okinawa trough during the late Quaternary. Palaeogeogr. Palaeoclimatol. Palaeoecol. 430, 74–84.
Li, Z., Peterse, F., Wu, Y., Bao, H., Eglinton, T.I., Zhang, J., 2015b. Sources of organic matter in Changjiang (Yangtze River) bed sediments: preliminary insights from organic geochemical proxies. Org. Geochem. 85, 11–21.
Li, F., Zheng, F., Wang, Y., Liu, W., Zhang, C.L., 2017. Thermoplasmatales and methanogens: potential association with the crenarchaeol production in Chinese soils. Front. Microbiol. 8, 1–13.
Liu, L., Chen, J., Ji, J., Chen, Y., 2004. Comparison of paleoclimatic change from Zr/Rb ratios in Chinese loess with marine isotope records over the 2.6-1.2 Ma Bp interval. Geophys. Res. Lett. 31, 383–402.
Liu, L., Chen, J., Ji, J., Chen, Y., Balsam, W., 2006. Variation of Zr/Rb ratios in the Chinese loess deposits during the past 1.8 Myr and its implication for the change of East Asian monsoon intensity. Geochem. Geophys. Geosyst. 7, 1–9.
Liu, J.P., Xu, K.H., Li, A.E.A., Milliman, J.D., Velozzi, D.M., Xiao, S.B., Yang, Z.S., 2007. Flux and fate of Yangtze River sediment delivered to the East China Sea. Geomorphology 85, 208–224.
Luo, C., Zheng, H.B., Wu, W.H., Wang, P., Chen, Y.L., Wei, X.C., 2012. Sr-Nd isotope stratification along water depth: an example from Datong hydrological station of Yangtze River. Chin. Sci. Bull. 57 (34), 4482–4490.
Lv, X.X., Yang, H., Song, J.M., Versteegh, G.J.M., Li, X.G., Yuan, H.M., Li, N., Yang, C.B., Yang, Y., Ding, W.H., Xie, S.C., 2014. Sources and distribution of isoprenoid glycerol dialkyl glycerol tetraethers (GDGTs) in sediments from the east coastal sea of China: application of GDGT-based paleothermometry to a shallow marginal sea. Org. Geochem. 75, 24–35.
Lv, X.X., Liu, X.L., Elling, F.J., Yang, H., Xie, S., Song, J., Li, X., Yuan, H., Li, N., Hinrichs, K.U., 2015. Hydroxylated isoprenoid GDGTs in Chinese coastal seas and their potential as a paleotemperature proxy for mid-to-low latitude marginal seas. Org. Geochem. 89, 31–43.
Macklin, M.G., Benito, G., Gregory, K.J., Johnstone, E., Lewin, J., Michczyńska, D.J., Soja, R., Starkel, L., Thorndycraft, V.R., 2006. Past hydrological events reflected in the Holocene fluvial record of Europe. Catena 66, 145–154.
Mao, C.P., Chen, J., Yuan, X.Y., 2010. Seasonal variation in the mineralogy of the suspended particulate matter of the lower Changjiang River at Nanjing, China. Clay Clay Miner. 58, 691–706.
Mao, C.P., Chen, J., Yuan, X.Y., Yang, Z.F., Ji, J.F., 2011. Seasonal variations in the Sr-Nd isotopic compositions of suspended particulate matter in the lower Changjiang River: provenance and erosion constraints. Chin. Sci. Bull. 56 (22), 2371–2378.
Meng, J., Yao, P., Bianchi, T.S., Li, D., Zhao, B., Xu, B., Yu, Z., 2015. Detrital phosphorus as a proxy of flooding events in the Changjiang River Basin. Sci. Total Environ. 517, 22–30.
Middelkoop, H., Erkens, G., Van der Perk, M., 2010. The Rhine delta-a record of sediment trapping over time scales from millennia to decades. J. Soils Sediments 10, 628–639.
Milliman, J.D., Farnsworth, K.L., 2013. River Discharge to the Coastal Ocean: A Global Synthesis. Cambridge University Press.
Olafsdottir, K.B., Schulz, M., Mudelsee, M., 2016. REDFIT-X: cross-spectral analysis of unevenly spaced paleoclimate time series. Comput. Geosci. 91, 11–18.
Paillard, D., Labeyrie, L., Yiou, P., 1996. Macintosh program performs time-series analysis. Eos. Trans. AGU 77, 379.
Pradhan, S., Zhang, J., Baskaran, M., Shirodkar, P.V., Wu, Y., Pradhan, U.K., 2017. Investigations of the spatial and temporal variations of Sr and Nd isotopes in sediments from two Indian rivers: implications to source identification. Geochem. Geophys. Geosyst. 18, 1520–1536.
Quinn, T.M., Taylor, F.W., Crowley, T.J., 2006. Coral-based climate variability in the Western Pacific Warm Pool since 1867. J. Geophys. Res. Oceans Atmos. 111 (C11006). https://doi.org/10.1029/2005JC003243.
Schouten, S., Huguet, C., Hopmans, E.C., Kienhuis, M.V.M., Sinninghe Damsté, J.S., 2007. Analytical methodology for TEX_{86} paleothermometry by high-performance liquid chromatography/atmospheric pressure chemical ionization-mass spectrometry. Anal. Chem. 79, 2940–2944.
Schouten, S., Hopmans, E.C., Sinninghe Damsté, J.S., 2013a. The organic geochemistry of glycerol dialkyl glycerol tetraether lipids: a review. Org. Geochem. 54, 19–61.
Schouten, S., Hopmans, E.C., Rosell-Melé, A., Pearson, A., Adam, P., Bauersachs, T., Bard, E., Bernasconi, S.M., Bianchi, T.S., Brocks, J.J., Carlson, L.T., Castañeda, I.S., Derenne, S., Selver, A.D., Dutta, K., Eglinton, T., Fosse, C., Galy, V., Grice, K., Hinrichs, K.U., Huang, Y., Huguet, A., Huguet, C., Hurley, S., Ingalls, A., Jia, G., Keely, B., Knappy, C., Kondo, M., Krishnan, S., Lincoln, S., Lipp, J., Mangelsdorf, K., Martínez-García, A., Ménot, G., Mets, A., Mollenhauer, G., Ohkouchi, N., Ossebaar, J., Pagani, M., Pancost, R.D., Pearson, E.J., Peterse, F., Reichart, G., Schaeffer, P., Schmitt, G., Schwark, L., Shah, S.R., Smith, R.W., Smittenberg, R.H., Summons, R.E., Takano, Y., Talbot, H.M., Taylor, K.W.R., Tarozo, R., Uchida, M., van Dongen, B.E., Van Mooy, B.A.S., Wang, J., Warren, C., Weijers, J.W.H., Werne, J.P., Woltering, M., Xie, S., Yamamoto, M., Yang, H., Zhang, C.L., Zhang, Y., Zhao, M., Sinninghe Damsté, J.S., 2013b. An interlaboratory study of TEX_{86} and BIT analysis of sediments, extracts, and standard mixtures. Geochem. Geophys. Geosyst. 14, 5263–5285.
Schulz, M., Stattegger, K., 1997. SPECTRUM: spectral analysis of unevenly spaced paleoclimatic time series. Comput. Geosci. 23, 929–945.
Shi, Y.F., Jiang, T., Su, B.D., Chen, J.Q., Qin, N.X., 2004. Preliminary analysis on the relation between the evolution of heavy floods in the Yangtze River catchment and the climate changes since 1840. J. Lake Sci. 16, 289–297 (in Chinese with English abstract).
Singh, S.K., Rai, S.K., Krishnaswami, S., 2008. Sr and Nd isotopes in river sediments from the Ganga Basin: sediment provenance and spatial variability in physical erosion. J. Geophys. Res. 113 (F03006).
Smith, J., Vance, D., Kemp, R.A., Archer, C., Toms, P., King, M., Zarate, M., 2003. Isotopic constraints on the source of Argentinian loess with implications for atmospheric circulation and the provenance of Antarctic dust during recent glacial maxima. Earth Planet. Sci. Lett. 212, 181–196.
Smith, R.W., Bianchi, T.S., Savage, C., 2010. Comparison of lignin phenols and branched/isoprenoid tetraethers (BIT index) as indices of terrestrial organic matter in Doubtful Sound, Fiordland, New Zealand. Org. Geochem. 41, 281–290.
Tanaka, T., Togashi, S., Kamioka, H., Amakawa, H., Kagami, H., Hamamoto, T., Yuhara, M., Orihashi, Y., Yoneda, S., Shimizu, H., Kunimaru, T., Takahashi, K., Yanagi, T., Nakano, T., Fujimaki, H., Shinjo, R., Asahara, Y., Tanimizu, M., Dragusanu, C., 2000. JNdi-1: a neodymium isotopic reference in consistency with LaJolla neodymium. Chem. Geol. 168, 279–281.
Tierney, J.E., Russell, J.M., 2009. Distributions of branched GDGTs in a tropical lake system: Implications for lacustrine application of the MBT/CBT paleoproxy. Org. Geochem. 40, 1032–1036.
Toonen, W.H.J., 2013. A Holocene Flood Record of the Lower Rhine. Utrecht University, Utrecht (Master Thesis).
Toonen, W.H.J., Kleinhans, M., Cohen, K., 2012. Sedimentary architecture of abandoned channel fills. Earth Surf. Process. Landf. 37 (4), 459–472.
Walling, D.E., 2005. Tracing suspended sediment sources in catchments and river systems. Sci. Total Environ. 344, 159–184.
Wang, M., Zheng, H., Xie, X., Fan, D., Yang, S., Zhao, Q., Wang, K., 2011. A 600-year flood

history in the Yangtze River drainage: comparison between a subaqueous delta and historical records. Chin. Sci. Bull. 56, 188–195.
Wei, G.J., Liang, Z., Deng, W.F., Li, X.H., Ying, L., Chen, J.F., 2009. Mn/Ca ratio in planktonic foraminifer from ODP site 1144, the northern South China Sea: a possible paleoclimate indicator. Geochem. J. 43, 235–246.
Weijers, J.W.H., Schouten, S., Hopmans, E.C., Geenevasen, J.A.J., David, O.R.P., Coleman, J.M., Pancost, R.D., Sinninghe Damsté, J.S., 2006. Membrane lipids of mesophilic anaerobic bacteria thriving in peats have typical archaeal traits. Environ. Microbiol. 8, 648–657.
Weijers, J.W.H., Schouten, S., van den Donker, J.C., Hopmans, E.C., Sinninghe Damsté, J.S., 2007. Environmental controls on bacterial tetraether membrane lipid distribution in soils. Geochim. Cosmochim. Acta 71, 703–713.
Wu, L., Wang, B., Geng, S., 2005. Growing typhoon influence on East Asia. Geophys. Res. Lett. 32, L18703. https://doi.org/10.1029/2005GL022937.
Xiao, M., Zhang, Q., Singh, V.P., 2015. Influences of ENSO, NAO, IOD and PDO on seasonal precipitation regimes in the Yangtze River Basin, China. Int. J. Climatol. 35 (12), 3556–3567.
Xing, L., Zhao, M., Gao, W., Wang, F., Zhang, H., Li, L., Liu, J., Liu, Y., 2014. Multiple proxy estimates of source and spatial variation in organic matter in surface sediments from the southern Yellow Sea. Org. Geochem. 76, 72–81.
Xu, K.Q., Chen, Z., Zhao, Y., Wang, Z., Zhang, J., Hayashi, S., Murakami, S., Watanabe, M., 2005. Simulated sediment flux during 1998 big-flood of the Yangtze (Changjiang) River, China. J. Hydrol. 308, 105–121.
Xu, K., Li, A., Liu, J.P., Milliman, J.D., Yang, Z., Liu, C.S., Kao, S.J., Wan, S., Xu, F., 2012. Provenance, structure, and formation of the mud wedge along inner continental shelf of the East China Sea: a synthesis of the Yangtze dispersal system. Mar. Geol. 291, 176–191.
Yang, S.Y., Jung, H.S., Li, C.X., 2004. Two unique weathering regimes in the Changjiang and Huanghe drainage basins: geochemical evidence from river sediments. Sediment. Geol. 164, 19–34.
Yang, S.Y., Jiang, S.Y., Ling, H.F., Xia, X.P., Sun, M., Wang, D.J., 2007. Sr-Nd isotopic compositions of the Changjiang sediments: implications for tracing sediment sources. Sci. China Ser. D Earth Sci. 50, 1556–1565.
Yang, H., Zhi, X.F., Gao, J., Liu, Y., 2011. Variation of East Asian summer monsoon and its relationship with precipitation of China in recent 111 years. Agric. Sci. Technol. 12, 1711–1716.
Yang, G., Zhang, C.L., Xie, S., Chen, Z., Gao, M., Ge, Z., Yang, Z., 2013. Microbial glycerol dialkyl glycerol tetraethers from river water and soil near the Three Gorges Dam on the Yangtze River. Org. Geochem. 56, 40–50.
Yang, S.L., Milliman, J.D., Xu, K.H., Deng, B., Zhang, X.Y., Luo, X.X., 2014. Downstream sedimentary and geomorphic impacts of the Three Gorges Dam on the Yangtze River. Earth-Sci. Rev. 138, 469–486.
Yang, S.L., Xu, K.H., Milliman, J.D., Yang, H.F., Wu, C.S., 2015a. Decline of Yangtze River water and sediment discharge: impact from natural and anthropogenic changes. Sci. Rep. UK 5. https://doi.org/10.1038/srep12581.
Yang, S.Y., Bi, L., Li, C., Wang, Z.B., Dou, Y.G., 2015b. Major Sinks of the Changjiang (Yangtze River)-Derived Sediments in the East China Sea During the Late Quaternary. Geological Society, London, pp. 429 (Special Publications).
Ypma, J., 2014. Using Chemical Composition and Grain Size Distribution of a Palaeochannel-Fill to Identify Lower Rhine Flood Events and Their Origin in the Catchment. Utrecht University, Utrecht (Master Thesis).
Yu, F., Chen, Z., Ren, X., Yang, G., 2009. Analysis of historical floods on the Yangtze River, China: characteristics and explanations. Geomorphology 113, 210–216.
Yu, Y., Song, J., Duan, L., Li, X., Yuan, H., Li, N., 2014. Sedimentary trace-element records of natural and human-induced environmental changes in the East China Sea. J. Paleolimnol. 52 (4), 277–292.
Yu, Z.T., Wang, X.J., Zhang, E.L., Zhao, C.Y., Liu, X.Q., 2015. Spatial distribution and sources of organic carbon in the surface sediment of Bosten Lake, China. Biogeosciences 74 (3), 13793–13817.
Yuan, S.Y., Zhao, X.A., Li, C.A., 2006. Identification marks of Paleoflood. Geol. Sci. Technol. Inf. 25, 55–58 (in Chinese with English abstract).
Zell, C., Kim, J.-H., Moreira-Turcq, P., Abril, G., Hopmans, E.C., Bonnet, M.-P., Sobrinho, R.L., Sinninghe Damsté, J.S., 2013. Disentangling the origins of branched tetraether lipids and crenarchaeol in the lower Amazon River: implications for GDGT-based proxies. Limnol. Oceanogr. 58, 343–353.
Zhang, J., 1999. Heavy metal compositions of suspended sediments in the Changjiang (Yangtze River) estuary: significance of riverine transport to the ocean. Cont. Shelf Res. 19, 1521–1543.
Zhang, R., Wang, Y.P., Pan, S.M., 2006. Analyses with wavelet and Hilbert-Huang transform on monthly water discharges at Datong station, Yangtze River. J. Nanjing Univ. 42, 423–434.
Zhang, R., Wang, Y.P., Gao, J.H., Pan, Shaoming, 2009. Sediment texture and grain-size implications: the Changjiang subaqueous delta. Acta Oceanol. Sin. 28, 38–49.
Zhao, Y., 2000. Thinking on the flood disaster in the middle reaches of the Yangtze River. Earth Sci. Front. 7, 87–93.
Zhao, G., Huang, G., Wu, R., Tao, W., Gong, H., Qu, X., Hu, K., 2015. A new upper-level circulation index for the East Asian Summer monsoon variability. J. Clim. 28, 9977–9996.
Zhao, Y., Zou, X., Gao, J., Wang, C., 2016. Recent sedimentary record of storms and floods within the estuarine-inner shelf region of the East China Sea. The Holocene 27, 439–449.
Zheng, J., Yamada, M., 2006. Inductively coupled plasma-sector field mass spectrometry with a high-efficiency sample introduction system for the determination of Pu isotopes in settling particles at femtogram levels. Talanta 69, 1246–1253.
Zhou, H., Hu, J., Spiro, B., Peng, P.A., Tang, J., 2014. Glycerol dialkyl glycerol tetraethers in surficial coastal and open marine sediments around China: Indicators of sea surface temperature and effects of their sources. Palaeogeogr. Palaeoclimatol. Palaeoecol. 395, 114–121.
Zhu, C., Weijers, J.W.H., Wagner, T., Pan, J., Chen, J., Pancost, R.D., 2011. Sources and distributions of tetraether lipids in surface sediments across a large riverdominated continental margin. Org. Geochem. 42, 376–386.
Zhu, C., Wagner, T., Talbot, H.M., Weijers, J.W.H., Pan, J.M., Pancost, R.D., 2013. Mechanistic controls on diverse fates of terrestrial organic components in the East China Sea. Geochim. Cosmochim. Acta 117, 129–143.